RESEARCH ARTICLE

Editorial Process: Submission:08/24/2024 Acceptance:12/020/2024

Dosimetric Evaluation of Different Algorithms on Heterogeneous Slab Phantom Using CMS XiO and MONACO Treatment Planning System for 4MV, 6MV and 15MV Beam Energy: An Institutional Study

Ajay Katake[1,2], Lalit Kumar[3], Balbir Singh[4], Nijun Mishra[5], Pradeep Gurjar[6], Rajesh Vashistha[6], Deepak Basandrai[1]*

Abstract

Aim: To study the dosimetric behavior of dose computational algorithms in inhomogeneous medium using CMS XiO and MONACO treatment planning system (TPS) for 4 megavoltage (MV), 6 MV and 15 MV photon beam energies. **Material and Methods:** Styrofoam blocks of thickness 1.90 cm, 3.8 cm and 5.70 cm was used to introduce inhomogeneity in a slab phantom. Wipro GE computed tomography (CT) scanner was used to scan the phantom. Doses were computed on the central axis of the beam using convolution (C), superposition (S), fast superposition (FS), collapsed cone convolution (CCC) and monte carlo (MC) algorithms for field geometries of 5x5 cm^2 and 10x10 cm^2 for above said photon beam energies, respectively. An Ion chamber (IC) of 0.6 cc volume was used for the dose measurements. The deviation between measured and TPS computed doses were recorded. **Results:** The PDD (Percentage depth dose) data obtained from the TPS (calculated data) and LINAC (measured data) was used for comparison based on different algorithms in order to calculate the percentage of maximum deviation (PMD). The PMD in MC algorithm were calculated for field sizes of 5x5 cm^2 and 10x10 cm^2 are found to be in ranging from 0.73% to -4.49% for 4MV, 1.62% to -2.42% for 6MV and 4.53% to -1.47% for 15 MV for 1.90 cm air gap, 2.21% to -3.75% for 4MV, 3.87% to -2.88% for 6 MV and 4.87% to -3.46% for 15 MV for 3.80 cm air gap, 2.77% to -4.66% for 4MV, 3.87% to -2.86% for 6 MV and 5.66% to -4.92% for 15 MV for 5.70cm air gap which is less as compared to CCC, C, FS, and S algorithms. **Conclusion:** The comparison of C, S, FS, CCC and MC algorithms demonstrated that MC having better agreement with IC measurements. In conclusion, MC is a superior option for dose computation, particularly in the presence of low-density heterogeneities.

Keywords: Convolution- Superposition- Fast Superposition- Collapsed Cone- Monte Carlo- air gap

Asian Pac J Cancer Prev, **25 (12)**, 4381-4389

Introduction

Advanced cancer treatment methods viz. intensity modulated radiation therapy (IMRT) and volumetric modulated arc therapy (VMAT) have made it possible to deliver conformal dose distribution to the target while reducing the dose to vital structures vicinity to the tumor. However, these sophisticated treatment methods also necessitate the use of treatment planning system (TPS) with more precise dose calculation algorithms [1]. The features of a therapeutic radiation beam will vary depending on the tissues it interacts inside the human body as it is made up of heterogeneous tissues such as bones, lungs, sinuses, oral and nasal cavities. Additionally, the immobilization device that holds the patient during treatment in place on the treatment table may generate an air gap through which the photon beam can travel [2]. Sometimes this gap perturbs the dose calculation that is why there is need of using appropriate algorithm. Commercially available TPSs are using various dose calculation algorithms that take into consideration the existence of various heterogeneity media, in order to accurately calculate the absorbed dose in the irradiated tissues having heterogeneous medium.

For dose calculation, Elekta medica system provides XiO and Monaco TPSs for radiation dose computation. For

*[1]Department of Physics, Lovely Professional University, Phagwara, India. [2]Department of Radiation Oncology, Samanvay Multispeciality Hospital PVT LTD, Junagadh, India. [3]Department of Radiation Oncology, Max Super speciality Hospital, Saket, India. [4]Department of Radiation Oncology, SLBSGMC & H, Nerchowk, Mandi, India. [5]Department of Radiation Oncology, GCRI-BCCRI, Bhavnagar, India. [6]Department of Radiation Oncology, Max Super Speciality Hospital, Bathinda, India. *For Correspondence: deepakbasandrai@gmail.com*

dose optimization, the XiO and MONOCO TPS utilizes The XiO (version 5.0) TPS utilizes Convolution (C), Superposition (S) and Fast Superposition (FS), Monaco (version 5.0) TPS utilizes Collapsed Cone Convolution (CCC) and Monte Carlo (MC) algorithms for dose computation, respectively [3].

The XiO Fast-Fourier Transform (FFT) Convolution (C) and Superposition (S) (Wiesmeyer and Miften) dose computation algorithms use the convolution of the TERMA (i.e., total energy released in the medium per unit mass) with energy deposition kernel (EDK). Kernel usually computed using monte-carlo simulation [4, 5].

TERMA is defined as following integrating over the beam spectrum [6],

$$T\ (r) = \int_E \frac{\mu}{\rho}\ (r, E)\varphi_E(r)dE$$

Where,

φ_E (r) is energy fluence, μ/ρ(r, E) is mass attenuation coefficient

TERMA coincide with absorbed dose for energy released locally absorbed. For secondary energy transport, dose can be computed in the media using the following convolution,

In homogeneous media,

$$D\ (r) = \int_E \int_V T_E\ (s)h(r - s, E)dsdE$$

Where,

h (s,E) is known as dose spread kernel (DSK), at energy E and position s relative to the point of scattering of the primary photon. It defines the energy transport by the secondary particles, including single and multiple scattered photons, photoelectric electrons, Compton electrons, electron–positron pairs, bremsstrahlung photons, photonuclear particles and so on.

In inhomogeneous media, the translation invariance is broken and a single DSK may no longer account for the secondary transport throughout the medium. Therefore, a full superposition integral need to be carried out [6]:

$$D\ (r) = \frac{1}{\rho(r)} \int_E \int_V T_E\ (s)\ \rho\ (s)k(r, s, E)dsdE$$

where,

k(r, s, E) is the normalized energy delivered at point r by secondary particles, associated to a primary photon of energy E interacting in s:

$$\int_V k(r, s, E)\ dr = 1$$

FFT Convolution Algorithm:

To execute the FFT convolution, the EDK defined by Mackie et al. must be interpolated from spherical to Cartesian coordinates on a common grid with the TERMA [5]. Steep kernel gradient complicates the sampling and interpolation of kernels from spherical to Cartesian coordinates. Adaptive quadrature techniques ensure that the correct energy at and near the interaction point is represented in the Cartesian coordinates. Sharpe and Battista and Mackie et al reported maximum volume used on XiO TPS, is about 30 cm in forward direction, 5 cm in backscatter direction and twice the field geometric dimension laterally for accurate dose estimation [7-9].

The XiO FFT C and S algorithms (Wiesmeyer and Miften) are algorithms are identical in nature. However, FFT C does not calculate dose as accurately as FFT S algorithm in the presence of tissue in-homogeneities [4].

Superposition Algorithm

The FFT S algorithm taken into account the variations in electron density, and based on ray tracing between the interaction and dose deposition sites, and scales the path length by density to get radiological path length between these sites. Hence the convolution equation which get modified for radiological path length is called the superposition equation. In superposition dose computation, the EDK can be modified to account for variations in electron density [6]. The XiO FFT S algorithm is an adaptation of "collapsed cone" dose calculation method [3]. Unlike FFT C algorithm, FFT S splits dose computation into two parts; primary kernel (for primary electron) and scatter kernel (for scattered photon).

Fast superposition algorithm

Spherical kernels, or "dose spread arrays", are cylindrically symmetric and defined in terms of rays traced along zenith and azimuth angles. The spherical kernel computation has been augmented with the ability to combine (select and sum) adjacent zenith rays in the kernel [3, 10]

Thus, for a trade-off between optimizing speed and accuracy, number and direction of the zenith rays are controlled. Higher zenith rays mean slower and more accurate computation and fewer zenith rays leads to fast and compromised accurate computation. For evenly-spaced azimuth angles, it is possible to control of both the direction and number of zenith and azimuth rays. The fast mode offers a fast Superposition dose computation with a factor of ~2.5 at the cost of minimal loss in accuracy, compared to the "standard" superposition calculation. Specifically, in few clinical scenarios, the fast Superposition dose is less accurate in terms of monitor units and dose compared to Superposition dose by 1-2%.

Collapsed Cone Convolution (CCC)

The CCC algorithm offers an efficient way to deal with DSK. In CCC, it is assumed that all the energy is released into the coaxial cones of equal solid angle. Further, it is transported rectilinearly, attenuated and deposited in elements on the axis. Inhomogeneity correction in the irradiated volume is performed using the density scaling of the kernel during convolution. The CCC offers good agreements with the measurements, except in low-density medium, where lateral charge particle equilibrium doesn't

exist [10].

Monte Carlo (MC)

The MC offers stochastic solution in simulation of the interaction between primary/secondary particle and media, by defining probability density distribution of the randomly sampled particle interaction history. Initial simulation uses pre-filled phase space of the beam line. Later particle path is divided into small steps of mean free path of the particle in the media. The amount of energy lost in each interaction and produced secondary particles, and their path along with subsequent interactions are recorded. This process is continued until each particle is locally deposited [6]. This simulation process has to be repeated N times to minimize the statistical uncertainty of the computation. This may lead to a vast computation depending upon the complexity and size of the geometry or desired accuracy. Finally, dose is calculated by summing the all-energy releases that occurred in each mass element of the media. GEANT, EGS, BEAM, PENELOPE and XVMC are the examples of MC code used in RT. Mass density, electron density and atomic composition are required to calculated radiation transport in the tissue [11-15].

Dose computation algorithm are well-known for their limitation in dealing with low-density interfaces. Kumar et al. highlighted the limitation of dose computation algorithm in dealing with low-density heterogeneities [16]. Rana et al. reported the limitation of dose computation in dealing with small lung tumors and air gaps created by immobilization tools [17]. Fogliata et al. investigated the behavior of dose algorithm in presence of simple geometric inhomogeneities and reported discrepancies amongst different algorithms for inhomogeneity of density of 0.035 g/cc [18]. Further, they concluded more enhanced discrepancies with increase in photon beam energies and decrease in field geometry.

The comparative study reported by Saini et al. using pencil beam convolution algorithm (PBC), Collapsed Cone Convolution (CCC) and Monte Carlo (MC) algorithm in the Monaco treatment planning system [19]. The investigations were mostly concentrated around the tissue heterogeneity interface in the comparison between TPS calculated and measured data, and it is yet unknown how accurately algorithms are predicting dose at many depths beyond various air gap widths. Accuracy of dose computation algorithm became of utmost importance for better therapeutic outcome in inhomogeneous medium in radiotherapy. Therefore, present study tries to explore the behavior of dose computation algorithm equipped in XiO and Monaco TPS under the effect of heterogeneous medium of varying thickness.

Present study uses C, S, FS equipped in XiO TPS, CCC and MC algorithms equipped in MONACO TPS for the dose calculations. The goal of this study is to investigate results of five different dose calculation algorithms at central axis depth dose with varying heterogeneity using three-dimensional conformal radiation therapy (3DCRT) techniques for three different photon energies. This study will also help medical physicists to determine which algorithm is appropriate for dose calculation in heterogeneous medium.

Materials and Methods

In order to introduce the inhomogeneity, rectangular Styrofoam cube of varying thickness was sandwiched between the slabs of solid water. First 5.0 cm solid water then cubes of Styrofoam (thickness of (a) 1.9 cm, (b) 3.8 cm and (c) 5.7 cm) to create air gap between slabs as shown in Figure. 1 followed by 10.0 cm of solid water slabs. Phantom was scanned on the Wipro GE computed tomography (CT) scanner and DICOM images were transferred to XiO and Monaco TPS shown in Figure 2. A slice thickness of 1 mm was used for CT scan with scanning parameters of 120 kVp, 80 mAs.

Elekta Synergy Platform linear accelerator (LINAC) was used to generate the photon beam of 4 MV, 6 MV and 15 MV energies, respectively. A source-to-surface (SSD) of 100 cm setup was used for the experiment purpose. The central axis dose was calculated using C, S, FS algorithm in XiO TPS and CCC, MC in Monaco TPS for the field geometries of 5 x 5 cm^2 and 10 x 10 cm^2, respectively. The calculation grid used was 3.0 mm x 3.0 mm x 3.0 mm. The dose calculated (a) before Styrofoam up to 4.0 cm from the top of the phantom's surface, and (b) beyond Styrofoam up to 10.0 cm from the Styrofoam/solid-slab phantom.

An Ion-chamber (IC) FC65G in combination with an electrometer was used to collect the charge produced at point of measurements. Later charge was converted to dose as per technical series report 398 (TRS-398) as prescribed by IAEA. The charge collected was converted to dose using the correction factor namely viz., temperature, pressure, ion-recombination, and polarization. IC was calibrated in a secondary standard laboratory for dose-to-water calibration factor, which was also applied to get dose from the collected charge.

Dose Comparison

The central axis dose (CAX) was calculated for field geometry of 5.0 cm x 5.0 cm and 10.0 cm x 10.0 cm under SSD setup for (a) 1.9 cm gap of air (b) 3.8 cm gap of air, and (c) 5.7 cm gap of air. IC measured dose were validated on the central axis against the computation of C, S, FS, CCC and MC algorithms using the following formulae.

$$Variation\ (in\ \%) = \frac{Dose_{Algorithm} - Dose_{IC}}{Dose_{Algorithm}} * 100$$

Results

The CAX data were measured for 5 x 5 cm^2 and 10 x 10 cm^2 field opening using 4, 6 and 15 MV photon beams. IC measured data and algorithm computed data were tabulated in Supplementary Tables 1,2, 3.

In first 5 cm of solid water (1.9cm air gap)

For 5 x 5 cm^2, the difference between IC measured and TPS computations were 1.37 to -4.0 %, 0 to -4.68%, 0 to -5.17%, 0.73 to -2.79 % and 2.52 to -3.99 % for 4 MV, similarly 0.25 to -0.94 % , 2.0 to -6.07 %, 1.85 to -1.25 % , 1.77 to -3.65 and 0.34 to -8.97 % for 6 MV, similarly, 2.74

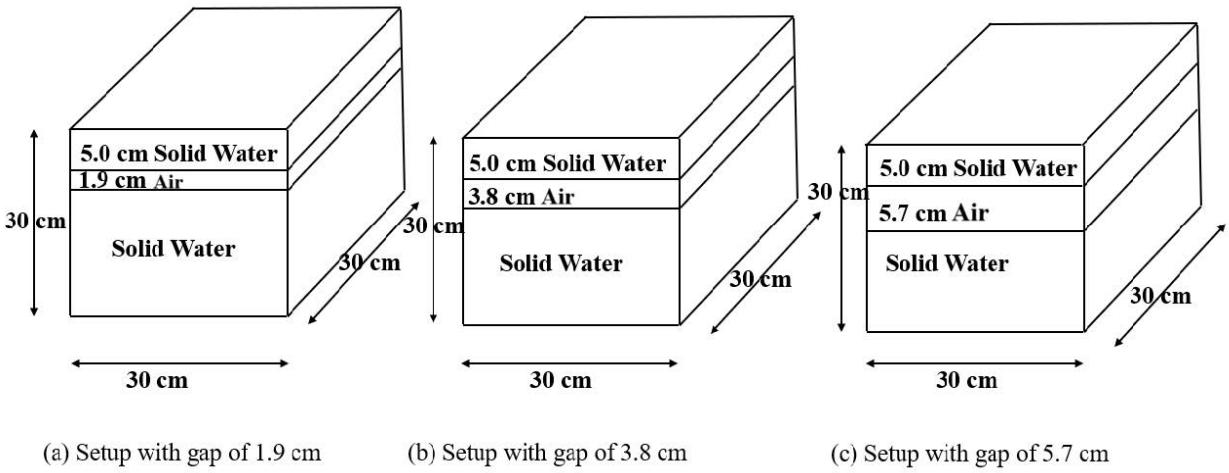

(a) Setup with gap of 1.9 cm (b) Setup with gap of 3.8 cm (c) Setup with gap of 5.7 cm

Figure 1. First 5.0 cm Solid Water then Cubes of Air to create air gap between slabs (thickness of (a) 1.9 cm, (b) 3.8 cm and (c) 5.7 cm followed by 10.0 cm of solid water slabs)

to -1.22%, 3.16 to -1.50%, 4.53 to -0.21, 0.12 to -1.46 %, and 6.93 to -0.60 for 15 MV using CCC, C , FS, MC and S dose computation algorithms, respectively.

For 10 x 10 cm^2, the difference between IC measured and TPS computations were 0.54 to 0 % , 0.96 to -0.96 %, 0 to -0.30 % , 0.10 to -0.44 and 0 to -0.42 for 4 MV, similarly 0.21 to -0.61 %, 0.0 to -0.92 %, 0.41 to -0.02 %, 0.00 to -0.21 and 0.96 to -0.10 for 6 MV, similarly, 0.00 to 0.20 %, 0.2 to 0 %, 0.70 to -0.81 %, 0 to -0.30 and 0.00 to -0.71 % for 15 MV using CCC, C , FS, MC and S dose computation algorithms, respectively.

In first 5 cm of solid water (3.8cm air gap)

For 5 x 5 cm^2, the difference between IC measured and TPS computations were 0.63 to -1.03 %, 0 to -5.05%, 0 to -1.91%, 0.7313o -0.64 % and 1.83 to -0.05 % for 4 MV, similarly 1.42 to -0.90 % , 2.26 to -1.30 %,0.66 to 0.0 % , 1.23 to -2.47 and 3.30 to -0.23 % for 6 MV, similarly, 1.26 to -1.27%, 2.75 to -1.55%, 0 to -1.73, 0.22 to -2.08 %, and 2.57 to -1.85 for 15 MV using CCC, C , FS, MC and S dose computation algorithms, respectively.

For 10 x 10 cm^2, the difference between IC measured and TPS computations were 1.6 to -3.67 % , -.95 to -7.29 %, -1.14 to -5.17 % , -1.52 to -2.86 and 6.80 to -3.19 for 4 MV, similarly 0.69 to -1.38 %, 0.53 to -4.24 %, 2.74 to -0.1 %, 2.29 to -2.55 and 5.42 to -0.42 for 6 MV, similarly, 2.72 to 0.00 %, 0.85 to -6.94 %, 0.79 to -2.36 %, 1.19 to -1.40 and 2.87 to -1.03 % for 15 MV using CCC, C , FS,

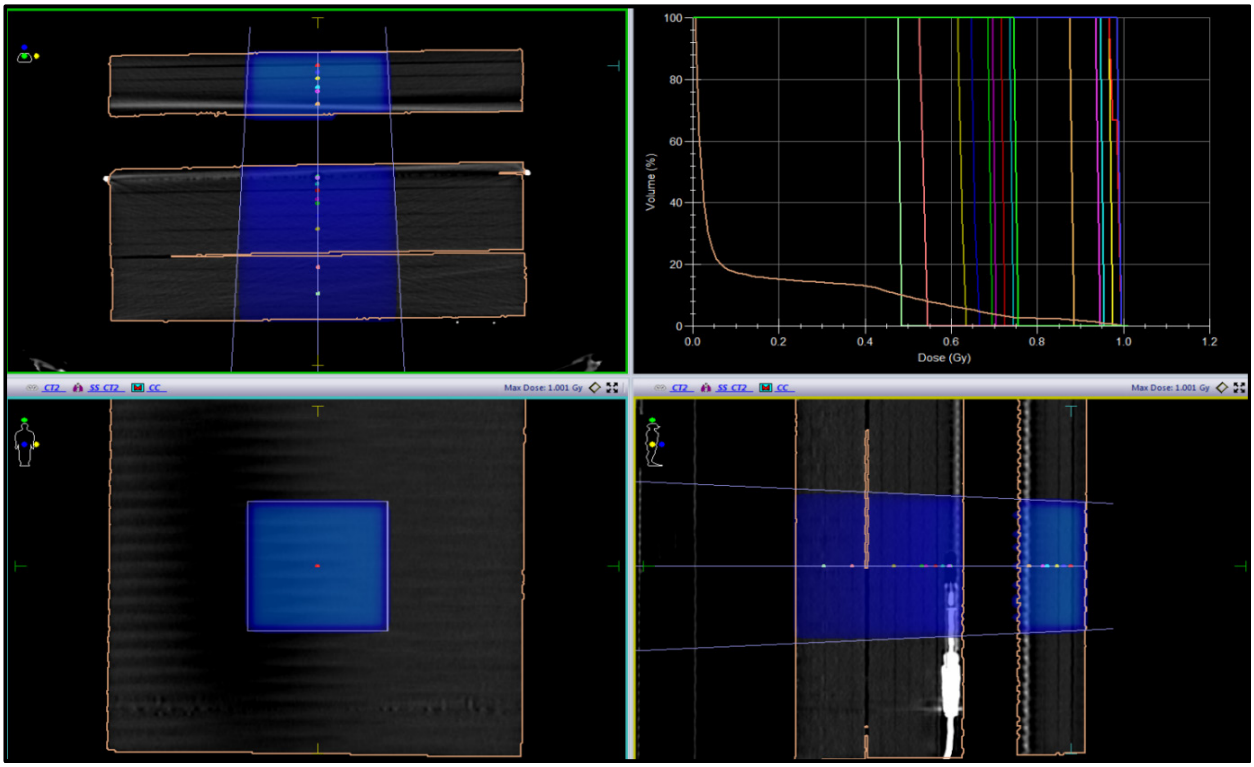

Figure 2. DICOM Images of Experimental Setup in TPS

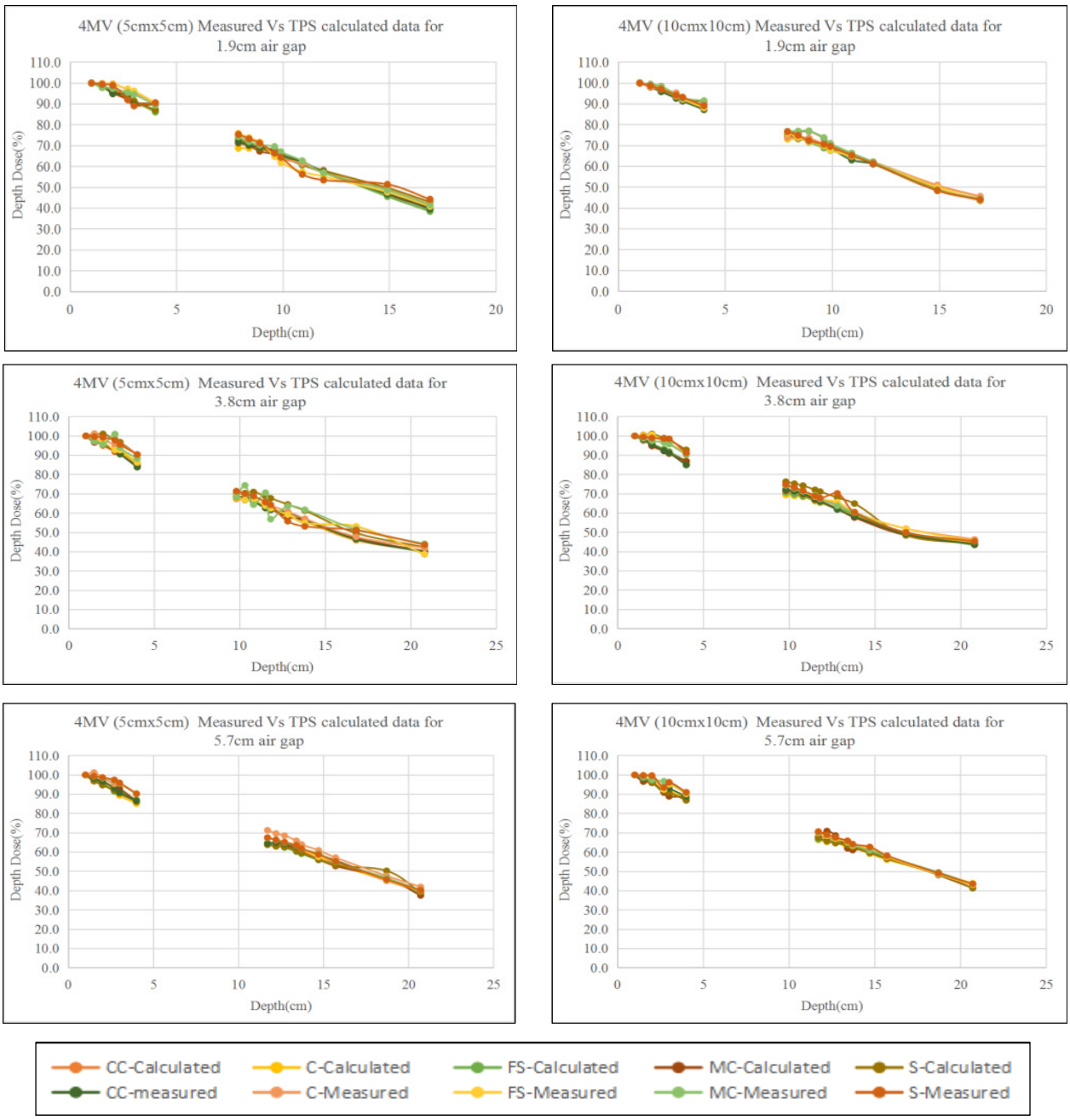

Figure 3. Illustrates the Observed PDDs as well as the Computed PDD Curves Using Algorithms in Phantoms A (1.9 cm air gap thickness), B (3.8cm air gap thickness), and C (5.7cm air gap thickness) for energy 4MV and field sizes 5X5 cm2, and 10X10 cm2and XIO TPS (C, S and FS) and Monaco TPS (CCC and MC).

MC and S dose computation algorithms, respectively.

In first 5 cm of solid water (5.7cm air gap)

For 5 x 5 cm^2, the difference between IC measured and TPS computations were 0.28 to -1.21 %, 0.00 to -7.07%, 0 to -6.5%, 0.53 to -1.42 % and 0.00 to -6.05 % for 4 MV, similarly 0.23 to -1.64 % ,0.00 to -6.37 %, 1.51 to -0.85 % , 0.89 to -1.98 and 1.59 to -4.16 % for 6 MV, similarly, 1.61 to -0.54%, 3.23 to -1.09%, 0.65 to -5.40, 1.99 to -1.20 %, and 0.88 to -0.17 for 15 MV using CCC, C , FS, MC and S dose computation algorithms, respectively.

For 10 x 10 cm^2, the difference between IC measured and TPS computations were 0.00 to -2.07 % , 0.00 to -4.61 %, 0 to -4.56 % , 0.00 to -2.90 and 0.00 to -5.79 for 4 MV, similarly 1.19 to -0.41 %, 6.71 to -0.82 %, 5.62 to -0.93 %, 0.53 to -1.43 and 6.81 to -0.71 for 6 MV, similarly, 1.32 to -1.08 %, 2.34 to -0.29%, 1.48 to -1.66 %, 1.76 to -2.21 and 0.00 to -2.81 % for 15 MV using CCC, C , FS, MC and S dose computation algorithms, respectively.

After air gap of 1.9 cm

For 5 x 5 cm^2, the difference between IC measured and TPS computations were 2.30 to -1.66 %, 2.86 to -9.67%, 5.22% to -6.19, 0.10 to -3.81 % and 8.18% to -3.50 for 4 MV, similarly 4.67 to -1.07 % , 2.76 to -10.05 %, 3.11 to -7.66 % , 2.94 to -3.26, and 1.62 to -3.07 % for 6 MV, similarly, 2.11 to -3.39 %, 3.18 to -8.12 %, 4.39 to -1.47 %, 3.17 to -2.83 %, 4.34 to -2.81 % for 15 MV using CCC, C , FS, MC and S dose computation algorithms, respectively.

For 10 x 10 cm^2, the difference between IC measured

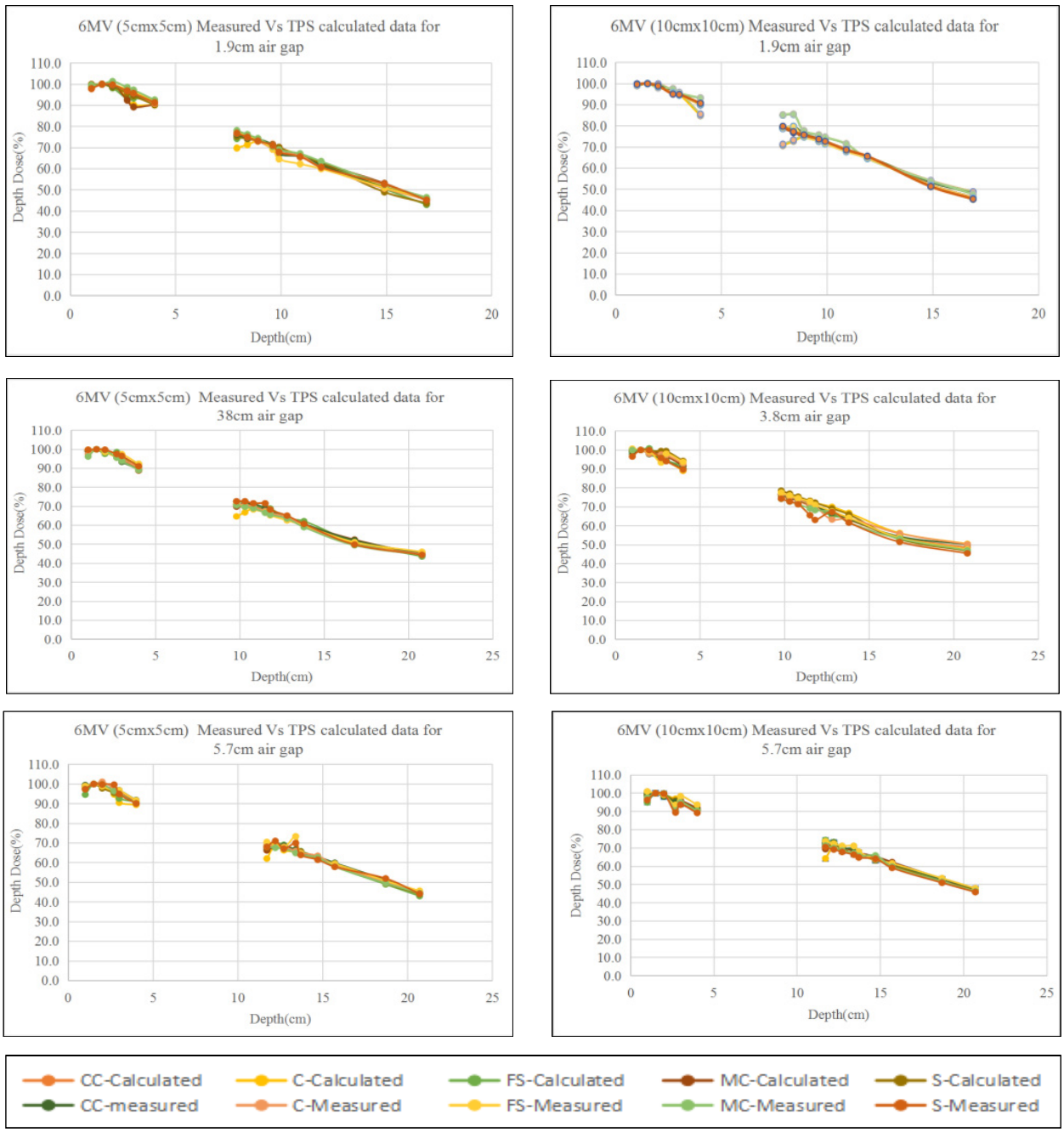

Figure 4. Illustrates the Observed PDDs as well as the Computed PDD Curves Using Algorithms in Phantoms C (5.7cm air gap thickness) for energy 6MV and field sizes 5X5 cm2, and 10X10 cm2and XIO TPS (C, S and FS) and Monaco TPS (CCC and MC).

and TPS computations were 3.06 to -0.03 %, -0.52 to -0.94 %, -0.30 to -1.48 %, -0.10 to -0.39 % and -0.12 to -0.58 % for 4 MV, similarly 0.55 to -0.97 %, -0.92% to -0.92, 0.62% to -3.69,, -0.21 to -0.21% and 0.45% to -0.34 for 6 MV, similarly, 1.01 to 0.20 %, 0.20 to 0.20 %, -0.08 to -2.71 %, -0.30 to -0.30 % and -0.20 to -1.19% for 15 MV using CCC, C , FS, MC and S dose computation algorithms, respectively.

After air gap of 3.8 cm

For 5 x 5 cm^2, the difference between IC measured and TPS computations were 1.36 to -2.16%, -2.20 to -5.28%, 2.82% to -13.51 %, 1.51% to -2.02% and 13.49% to -2.99% for 4 MV, similarly 0.99% to -1.99%, 1.36% to -10.47%, 3.34% to -4.01%, 2.69% to -0.62 % and 5.75% to -1.02% for 6 MV, similarly, 2.07% to -0.74 %, 3.34% to -8.70 %, 5.01% to -1.26%, 2.82% to -2.00 %, and 6.33 % to -2.62% for 15 MV using CCC, C , FS, MC and S dose computation algorithms, respectively.

For 10 x 10 cm^2, the difference between IC measured and TPS computations were 1.16 to -3.67%, -1.95 to -7.29%, -1.14% to -5.17 %, -1.52% to -2.86% and 6.80% to -3.19% for 4 MV, similarly -0.49% to -3.14%, 9.57% to -0.72%, 4.35% to -2.98%, 0.74% to -1.23 % and 12.67% to 2.65% for 6 MV, similarly, 3.58% to 0.30%, 0.79% to -5.07%, 5.01% to -2.92%, 2.85% to -2.70 %, and 4.87% to 0.30% for 15 MV using CCC, C , FS, MC and S dose computation algorithms, respectively.

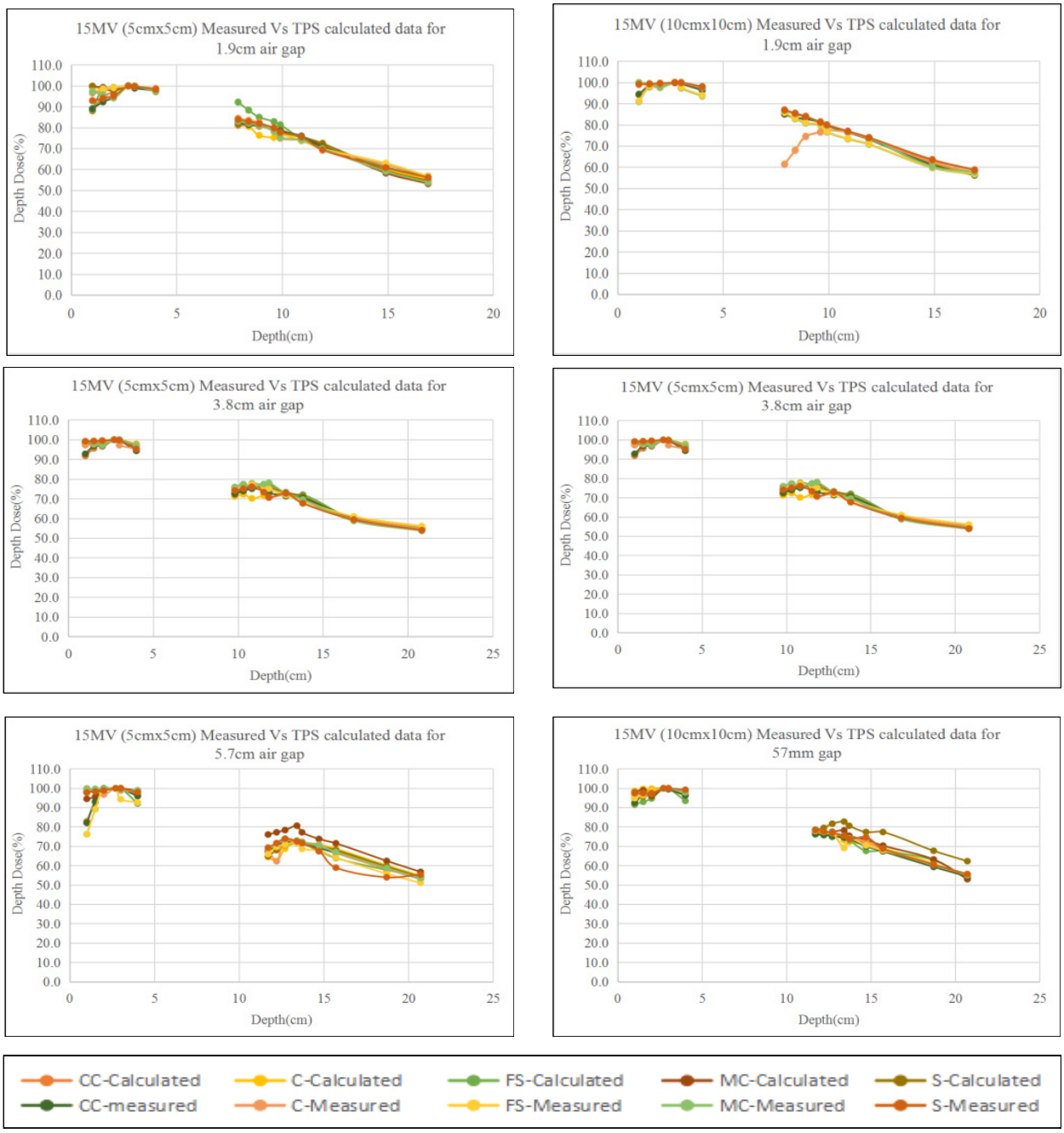

Figure 5. Illustrates the Observed PDDs as well as the Computed PDD Curves Using Algorithms in Phantoms C (5.7cm air gap thickness) for energy 15MV and field sizes 5X5 cm2, and 10X10 cm2and XIO TPS (C, S and FS) and Monaco TPS (CCC and MC).

After air gap of 5.7 cm

For 5 x 5 cm^2, the difference between IC measured and TPS computations were for -1.15 to -3.08%, -4.34 to -11.73 %, 1.10 to -5.29 %, 0.61% to -3.01% and 9.01% to -5.78% for 4 MV, similarly 0.56% to -3.32%, 1.19% to -11.09%, 2.08% to -2.66%, 1.79% to -2.65%, and 2.51% to -5.05% for 6 MV, similarly, 2.17% to -2.16%, 3.21% to -6.50%, 9.43% to 4.66%, 2.91 to -1.01%, and 13.31% to -6.86% for 15 MV using CCC, C , FS, MC and S dose computation algorithms, respectively.

For 10 x 10 cm^2, the difference between IC measured and TPS computations were -0.93 to -3.32%, 0.83% to -6.43%, 1.85% to -5.05%, 2.89% to -3.03%, and -1.26% to -5.29% for 4 MV, similarly 1.76% to -2.01%, 3.04% to -10.75%, 3.87% to -2.86%, -0.66% to -1.74 %, and 3.54% to -0.71 % for 6 MV, similarly, 2.37% to 0.03%, 5.49% to -3.40%, 4.41% to -4.98%, 0.74% to -2.34%, 11.16% to 0.09% for 15 MV using CCC, C , FS, MC and S dose computation algorithms, respectively.

The observed PDDs as well as the computed PDD curves using algorithms in phantoms A (1.9cm air gap thickness), B (3.8cm air gap thickness), and C (5.7cm air gap thickness) for energies 4MV, 6MV and 15MV and field sizes 5X5 cm^2, and 10X10 $cm^2$and XIO TPS (C, S and FS) and Monaco TPS (CCC and MC) as shown in Figures 3,4,5.

Discussion

It is important to comprehend the advantages and disadvantages of every single algorithm because the performance and quality of a TPS are based on the various types of algorithms utilized at various planning system. In our investigation, we employed five different algorithms and try to determine which algorithm is best for calculating dose at the air-water interface and treating patients.

The dose estimation performance of MC over various air gap widths in basic geometric scenarios was assessed by comparing computed C, S, FS, and CCC algorithm data to experimental observed data for 4 MV, 6 MV, and 15 MV photon beam. The findings of this experiment showed that MC performed better in dose computation across air gaps/cavities than C, S, FS and CCC when compared to measurements, regardless of the energy used, field size selected, or air gap introduced. The results of this study suggest that MC is a superior method for calculating dose, particularly in the presence of low-density inhomogeneity. This type of experiment work evaluates the intrinsic limitations of a dose computation algorithm and help to make a better choice to compute the dose precisely.

In present study, there was no trend found for any dose algorithms in post air gap region. This can be attributed using the fact that there is difference lateral spreads of secondary electron produced in low-density region, and different approach used by various algorithm in modelling these secondary electron leads to difference in the computation data.

Muralidhar et al. investigated the C, S and FS algorithms for various treatment cites (lung, prostate, esophagus, hypopharynx) and concluded that care should be taken while making the choice for the algorithm because it can lead to significant alteration in the treatment outcomes [20]. Verma et al. recommended the MC over the PB (Pencil Beam), C, FS, S algorithm for the treatment of lung cancer [21]. They reported the over-estimation of doses to target as well as OAR's with significant alternation in dose to bony and air tissue parts for C compared to FS, S for breast radiotherapy [22].

Chaikh et al. highlighted the need of validation of algorithms in local clinic and proposed the formulism to provide the highest probability of decease cure, with the lowest toxicity to OAR's and lower morbidity [23]. Further, Chaikh et al. and Lalit et al. highlighted that with the upgrade in TPS software, there can be a dosimetric shift of more than 5-10 % for newer version of algorithm from its older version [23, 24]. TPS is a significant source of error, contributing up to 50% of the total errors that may lead to the deviation between planned and measured dose [25-27]. ICRU reported that majority of RT failure is related to geometric miss in target delineation and dosimetric issues of more than ± 3% [28]. It has been proven that for 1 % improvement in overall accuracy, there is two-fold increase in treatment outcome [29].

Hence, based on the study, it can be concluded that MC has better agreement with IC measured data compared to other algorithm used in the study, regardless of photon energy, air-gaps used with different beam openings.

In conclusion, the dose estimation performance of MC over various air gap widths in basic geometric scenarios was assessed by comparing computed C, S, FS, and CCC algorithm data to experimental observed data for a 4 MV, 6 MV, and 15 MV photon beam. The findings of this experiment showed that MC performed better in dose computation across air gaps/cavities than C, S, FS and CCC when compared to measurements. The results of this study suggest that MC is a superior method for calculating dose, particularly in the presence of low-density inhomogeneity. When using reduced field sizes for radiation treatment, care must be taken to eliminate excessive air gaps caused by immobilization devices. As a result, we recommend that each beam data set and algorithm undergo a detailed examination of the accuracy for dose calculations in heterogeneous media.

Author Contribution Statement

All authors contributed equally in this study.

Acknowledgements

The authors wish to thanks Ms. Manpreet Kaur, Medical Physicist, Max Superspeciality Hospital, Bathinda for their support in taking measurements.

There are no sources in the current document. Used to investigate, write, analyse, preparation of figure and drafted the manuscript. Lalit Kumar, Pradeep Kumar, Balbir Singh, Nijun Mishra and Rajesh Vashistha contributed for conceptualization, analysis, methodology. Deepak Basandrai worked as a supervisor in-charge. The manuscript was reviewed by all of the authors.

Availability of Data

All data that support the findings of this study are included within the article.

Ethical Approval

Not Applicable because the study did not contain any human or animal studies.

Conflicts of Interest

None.

References

1. Rana S, Pokharel S. Verification of dose calculation algorithms in a multi-layer heterogeneous phantom using films. Gulf J Oncolog. 2013;1(14):63-9.
2. Papanikolaou N, Battista JJ, Boyer AL, Kappas C, Klein E, Mackie TR. AAPM report 85: Tissue Inhomogeneity Corrections for Megavoltage Photon Beams. Report of the AAPM radiation therapy committee task group 65. Delta. 2004 Jan 1. 136 p.
3. Animesh. Advantages of multiple algorithm support in treatment planning system for external beam dose calculations. J Cancer Res Ther. 2005;1(1):12–20. https://doi.org/10.4103/0973-1482.16085
4. Wiesmeyer MD, Miften MM. A multigrid approach for accelerating three-dimensional photon dose calculation. Med Phys. 1999;26:1149.

5. Mackie TR, Bielajew AF, Rogers DW, Battista JJ. Generation of photon energy deposition kernels using the EGS Monte Carlo code. Phys Med Biol. 1988;33:1-20. https://doi.org/10.1088/0031-9155/33/1/001
6. De Martino F, Clemente S, Graeff C, Palma G, Cella L. Dose calculation algorithms for external radiation therapy: An overview for practitioners. Appl Sci. 2021;11:6806. https://doi.org/10.3390/app11156806.
7. Sharpe MB, Battista JJ. Dose calculations using convolution and superposition principles: The orientation of dose spread kernels in divergent X-ray beams. Med Phys. 1993;20:1685-94. https://doi.org/10.1118/1.596955
8. Mackie TR, El-Khatib E, Battista J, Scrimger JW, Van Dyk J, Cunningham JR. Lung dose corrections for 6- and 15-MV X-rays. Med Phys. 1985;12:327-32. https://doi.org/10.1118/1.595691
9. Mackie TR, Scrimger JW, Battista JJ. A convolution method of calculating dose for 15 MV X-rays. Med Phys. 1985;12:188-96. https://doi.org/10.1118/1.595774
10. Ahnesjö A. Collapsed cone convolution of radiant energy for photon dose calculation in heterogeneous media. Med Phys. 1989;16:577–92. https://doi.org/10.1118/1.596360
11. GEANT4. Available from: https://geant4.web.cern.ch/support/user_documentation (Accessed on 2023 Dec 21).
12. Kawrakow I. Accurate condensed history Monte Carlo simulation of electron transport. I. EGSnrc, the new EGS4 version. Med Phys. 2000;27:485–98. https://doi.org/10.1118/1.598917
13. Rogers DW, Faddegon BA, Ding GX, Ma CM, We J, Mackie TR. BEAM: A Monte Carlo code to simulate radiotherapy treatment units. Med Phys. 1995;22:503–24. https://doi.org/10.1118/1.597552
14. Baro J, Sempau J, Fernández-Varea J, Salvat F. PENELOPE: An algorithm for Monte Carlo simulation of the penetration and energy loss of electrons and positrons in matter. Nucl Instrum Methods Phys Res Sect B Beam Interact Mater At. 1995;100:31–46.
15. Kawrakow I, Fippel M. Investigation of variance reduction techniques for Monte Carlo photon dose calculation using XVMC. Phys Med Biol. 2000;45:2163–83. https://doi.org/10.1088/0031-9155/45/8/308
16. Kumar L, Yadav G, Kishore V, Bhushan M. Dosimetric validation of Acuros XB photon dose calculation algorithm on an indigenously fabricated low-density heterogeneous phantom. Radiat Prot Environ. 2019;42:173–9.
17. Rana S, Rogers K. Dosimetric evaluation of Acuros XB dose calculation algorithm with measurements in predicting doses beyond different air gap thickness for smaller and larger field sizes. J Med Phys. 2013;38(1):9. https://doi.org/10.4103/0971-6203.106600
18. Fogliata A, Vanetti E, Albers D, Brink C, Clivio A, Knöös T, et al. On the dosimetric behaviour of photon dose calculation algorithms in the presence of simple geometric heterogeneities: comparison with Monte Carlo calculations. Phys Med Biol. 2007;52(5):1363. https://doi.org/10.1088/0031-9155/52/5/011.
19. Saini A, Pandey VP, Singh A, Kumar P. Evaluating impact of medium variation on dose calculated through planning system in a low-cost in-house phantom. Biomed Phys Eng Express. 2022;8(2):25022. https://doi.org/10.1088/2057-1976/ac53bc
20. Muralidhar K, Murthy N, Raju A, Sresty NVNM. Comparative study of convolution, superposition, and fast superposition algorithms in conventional radiotherapy, three-dimensional conformal radiotherapy, and intensity-modulated radiotherapy techniques for various sites, done on CMS XIO planning system. J Med Phys. 2009;34(1):12–22. https://doi.org/10.4103/0971-6203.48716
21. Verma T, Painuly NK, Mishra SP, Shajahan M, Singh N, Bhatt ML, et al. Performance evaluation of algorithms in lung IMRT: A comparison of Monte Carlo, Pencil Beam, Superposition, Fast Superposition, and Convolution Algorithms. J Biomed Phys Eng. 2016;6(3):127–138.
22. Gaur G, Dangwal VK, Banipal RPS, Singh R, Kaur G, Grover R, et al. Dosimetric comparison of different dose calculation algorithms in postmastectomy breast cancer patients using conformal planning techniques. J Med Phys. 2023;48(2):136–145. https://doi.org/10.4103/jmp.jmp_28_23.
23. Chaikh A, Ojala J, Khamphan C, Garcia R, Giraud JY, Thariat J, et al. Dosimetrical and radiobiological approach to manage the dosimetric shift in the transition of dose calculation algorithm in radiation oncology: how to improve high-quality treatment and avoid unexpected outcomes? Radiat Oncol. 2018;13(1):60. https://doi.org/10.1186/s13014-018-1005-2.
24. Kumar L, Bhushan M, Kishore V, Yadav G, Gurjar OP. Dosimetric validation of Acuros® XB algorithm for RapidArc™ treatment technique: A post software upgrade analysis. J Cancer Res Ther. 2021;17(6):1491–98. https://doi.org/10.4103/jcrt.JCRT_1154_19.
25. Ezzell GA, Burmeister JW, Dogan N, LoSasso TJ, Mechalakos JG, Mihailidis D, et al. IMRT commissioning: Multiple institution planning and dosimetry comparisons, a report from AAPM Task Group 119. Med Phys. 2009;36:5359–73. https://doi.org/10.1118/1.3238104
26. Ibbott GS, Followill DS, Molineu HA, Lowenstein JR, Alvarez PE, Roll JE. Challenges in credentialing institutions and participants in advanced technology multi-institutional clinical trials. Int J Radiat Oncol Biol Phys. 2008;71(1 Suppl):S71–5. https://doi.org/10.1016/j.ijrobp.2007.08.083
27. Kumar L, Yadav G, Kishore V, Bhushan M, Gairola M, Tripathi D. Validation of the RapidArc Delivery System Using a Volumetric Phantom as Per Task Group Report 119 of the American Association of Physicists in Medicine. J Med Phys. 2019;44(2):126–134. https://doi.org/10.4103/jmp.JMP_118_18.
28. Chetty IJ, Curran B, Cygler JE, DeMarco JJ, Ezzell G, Faddegon BA, et al. Report of the AAPM Task Group No. 105: Issues associated with clinical implementation of Monte Carlo-based photon and electron external beam treatment planning. Med Phys. 2007;34:4818–53. https://doi.org/10.1118/1.2795842
29. Boyer AL, Schultheiss T. Effects of dosimetric and clinical uncertainty on complication-free local tumor control. Radiother Oncol. 1988;11:65 71. https://doi.org/10.1016/0167-8140(88)90046-1